Characterization of thickness variations of thin dielectric layers at the nanoscale using scanning capacitance microscopy

V. Yanev,[a] M. Rommel, and A. J. Bauer
Fraunhofer Institute for Integrated Systems and Device Technology (IISB), Schottkystrasse 10, 91058 Erlangen, Germany

L. Frey
Fraunhofer Institute for Integrated Systems and Device Technology (IISB), Schottkystrasse 10, 91058 Erlangen, Germany and Chair of Electron Devices, University of Erlangen-Nuremberg, Cauerstrasse 6, 91058 Erlangen, Germany

(Received 10 August 2010; accepted 6 December 2010; published 6 January 2011)

In this work, the applicability of scanning capacitance microscopy (SCM) for film thickness characterization and its sensitivity to the surface roughness on nanoscale were examined experimentally. SiO_2 layers with different film thicknesses (between 5 and 19 nm) were analyzed by conventional capacitance-voltage (*C-V*) measurements and using SCM in the scanning capacitance spectroscopy (SCS) mode. The influence of the film thickness on the SCM signal was studied in detail by comparison of modeled data with experimental data. The dC/dV-V characteristics measured by SCS at the nanoscale could be correlated with derivatives of conventionally measured *C-V* curves as well as simulated *C-V* characteristics for the different film thicknesses. Quantitatively comparing their peak areas, it was found that the dC/dV signal of SCS correlates with the change in the insulator thickness. The sensitivity of SCM for the detection of local variations of dielectric-layer thicknesses at the nanoscale was demonstrated by SCM mapping of crystalline high-*k* layers, where spatial differences of the SCM signal could be directly correlated with changes in the topography caused by film thickness variations. © *2011 American Vacuum Society.* [DOI: 10.1116/1.3532822]

I. INTRODUCTION

Scanning capacitance microscopy (SCM) was developed for two-dimensional carrier profiling of cross-sectioned semiconductor samples at the nanoscale.[1–3] In that application, the change in capacitance ($\Delta C/\Delta V$), typically referred to as dC/dV of the local metal-insulator-semiconductor (MIS) capacitor (which is formed by the conductive tip, an insulator, and the semiconductor) is mainly related to the carrier concentration, assuming uniform insulator characteristics (especially with respect to interface state density, film homogeneity, and smoothness).

However, as the SCM signal is proportional to the change in capacitance (dC/dV) of the local MIS capacitor, it also strongly depends on the properties of the insulating layer. Some groups have exploited this fact and used SCM as a tool for nondestructive characterization of insulating layers on semiconductors.[4–10] There, when the underlying semiconductor shows homogeneous characteristics (i.e., doping concentration), the SCM output signal depends only on the insulator properties (layer thickness t_i, interface state density D_{it}, insulator charge Q_{Is}, and permittivity ε). The potential of SCM to analyze D_{it} and Q_{Is} for smooth SiO_2 and high-*k* layers has recently been investigated using scanning capacitance spectroscopy [SCS, i.e., measurements of local dC/dV versus voltage (dC/dV-V) characteristics)].[4–9] Higher interface trap densities lead to a broadening of the dC/dV peaks in the dC/dV-V curves. As suggested by Bowallius and Anand,[5] the full-width at half-maximum of the dC/dV peak can be used as a qualitative measure of D_{it}, whereas the charge density Q_{Is} and charge-trapping phenomena can be evaluated from the relative position of the dC/dV peak (i.e., the peak voltage). The capability of SCM to detect changes in film thickness for thick SiO_2 layers (20 and 50 nm) was also demonstrated.[10] No detailed knowledge, however, has been gained with respect to the influence of t_i on the SCM signal for thin layers (with a film thickness below 20 nm) and to the sensitivity of SCM for resolving small variations in t_i.

Especially for dielectric layers such as high-*k* films with large nonuniformities based on inhomogeneities in morphology (i.e., amorphous and/or crystalline phases in one layer depending on process conditions), this may be of great importance. Here, surface roughness may change significantly with film morphology and thickness. Specifically, as the SCM signal is directly proportional to the differential capacitance and it is higher for thinner films (e.g., the capacitance is inversely proportional to the insulator thickness), rougher film surfaces at still constant smooth interfaces will vary the insulator thickness for ultrathin layer more significantly and also the SCM signal.

In this work, the capability of SCM to detect changes in film thickness was studied. The SCM signal behavior and its dependence on the film thickness were particularly analyzed by comparison of SCS data with simulated and conventionally measured capacitance-voltage (*C-V*) characteristics for

[a]Electronic mail: vasil.yanev@iisb.fraunhofer.de

films with different SiO_2 thicknesses (5.3, 9.6, 14.5, and 19.0 nm). In addition, the relationship between SCM signal and surface roughness caused by spatial variation in film thickness was demonstrated by SCM mapping on relatively rough surfaces of crystalline ZrO_2 films.

II. EXPERIMENT

In order to examine the influence of t_i on the SCM signal, special SiO_2 samples were prepared where regions (stripes) with different thicknesses of 5.3, 9.6, 14.5, and 19.0 nm, respectively, were produced on the same Si substrate (p-type, specific resistance of 1–6 Ω cm) using multiple hydrofluoric acid etching steps. The original SiO_2 layer of 19.0 nm thickness was grown by dry oxidation. SiO_2 was chosen as the dielectric layer because of relatively low interface state densities, high surface smoothness, and consistent film thickness homogeneity. The root mean square (rms) roughness values for all examined thicknesses obtained from atomic force microscopy (AFM) measurements in tapping mode were about 0.2 nm. Homogeneous film thicknesses were determined by ellipsometry for all SiO_2 stripes. The wafer was cleaved into two pieces. On one piece, gate contacts consisting of 20 nm TiN and 300 nm Al stacks were patterned by photolithography and dry etching to form MIS capacitors. Finally, a forming-gas anneal at 430 °C for 30 min was performed for both samples.

Conventional C-V measurements in darkness were conducted on MIS capacitor structures with gate areas of 0.01 mm^2 using an impedance measuring instrument (LCZ meter HP 4277A). An alternating current (ac) frequency of 10 kHz and an effective voltage sweep V_{sw} of 0.02 V/s were set up for all measurements. Oscillation amplitudes V_{ac} of both 56 mV and 1.5 V (peak to peak) were applied in the experiments. For each film thickness, theoretical ideal C-V curves were calculated[11] with 0 V flat-band voltage, no D_{it}, no Q_{Is}, and doping concentration of 4×10^{15} cm^{-3}. These simulated ideal curves were also modulated with a ΔV of 1.5 V. In addition, dC/dV-V spectroscopy and SCM mapping were performed using a Veeco Dimension 5000 tool equipped with a Veeco SCM module (based on the RCA VideoDisc sensor[12]) and Pt/Ir coated silicon tips (nominal tip radius of about 20 nm) on the samples without the gate structures. SCM maps were performed at the transition regions between two SiO_2 thicknesses. The dC/dV-V curves were recorded at an ac frequency of 10 kHz and an ac amplitude V_{ac} of 1.5 V (peak to peak) as the sample bias voltage (tip always grounded) was swept from accumulation (+3 V sample bias) to inversion (−3 V sample bias) with a sweep rate V_{sw} of 0.05 V/s. A V_{sw} of 0.02 V/s (comparable to the V_{sw} used in the conventional C-V measurements) did not lead to any significant change in the recorded dC/dV-V curves with respect to the used V_{sw} of 0.05 V/s. The relatively high V_{ac} of 1.5 V and the ac frequency of 10 kHz were set up in order to achieve higher signal levels and a better signal-to-noise ratio, as especially for the thicker films, lower V_{ac} leads to very low signal-to-noise ratios. During sweeping, the AFM laser was switched off to ensure comparable conditions to conventional C-V measurements.

In addition, to study the sensitivity of the SCM signal on the surface roughness, crystalline high-k ZrO_2 layers with a thickness of about 10 nm were deposited by atomic-layer deposition on a p-type silicon wafer covered with a 1 nm Si_xN_y layer (rms roughness value below 0.2 nm) as the interface layer. After a postdeposition anneal at 1000 °C for 60 s, the films became nanocrystalline, with a resulting rms roughness of the ZrO_2 surface of about 0.85 nm. High-resolution transmission-electron microscopy (HR-TEM) images were obtained by an FEI CM 300 to analyze the ZrO_2 film properties (e.g., thickness, morphology, interface, and surface uniformity). Finally, the ZrO_2 samples were characterized by SCM mapping.

III. RESULTS AND DISCUSSION

A. Influence of stray capacitance on the SCM signal

The capacitance of the local MIS structure formed by the conductive tip, the dielectric layer, and the semiconductor (C_{tip}) has a maximum value typically in the range of 10–40 aF.[13] However, the SCM signal is affected by stray capacitance (C_{stray}) between the surface of the sample and the sensing probe (cantilever and body).[13–16] C_{stray} strongly disturbs or even dominates the signal under investigation. In fact, C_{stray} is typically in the range of 0.2 pF but strongly varies with the lateral and vertical probe positions[13] and may achieve values larger than 1 pF.[16] This influences the intensity of the SCM output signal, affects the capacitance sensor sensitivity, and hampers the quantitative evaluation when measurements are performed on locations relatively far from each another.[13] Therefore, quantitative interpretation of SCM results is challenging and often not very meaningful even in the presence of calibration data.

Since C_{tip} and C_{stray} are coupled in parallel,[13] the effective capacitance corresponds to the sum of both capacitances,

$$C_{eff} = C_{tip} + C_{stray}. \tag{1}$$

An analytic expression of the output voltage of the capacitance sensor,[12,17,18] typically referred to as dC/dV is given as follows:

$$V_{sensor} = \left| \beta \frac{f}{C_{eff}} \left(\frac{dC_{eff}}{dV} \bigg|_{V_{dc}} \right) \Delta V_{ac} \right|, \tag{2}$$

where β is a constant which can be determined by experiment, C_{eff} is the effective capacitance, and f is the drive frequency.[17] In a first approximation, considering Eqs. (1) and (2), the SCM output signal can be described as follows:

$$V_{sensor} \sim \frac{1}{C_{eff}} \frac{dC_{eff}}{dV} \approx \frac{1}{C_{tip}+C_{stray}} \frac{d(C_{tip}+C_{stray})}{dV}$$
$$\approx \frac{1}{C_{tip}+C_{stray}} \left(\frac{dC_{tip}}{dV} + \frac{dC_{stray}}{dV} \right). \tag{3}$$

Assuming that C_{stray} is much larger than C_{tip} and that

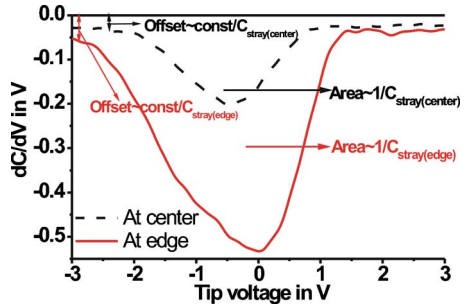

FIG. 1. (Color online) Influence of C_{stray} on the SCM output signal: dC/dV-V curves measured on different locations of the stripe with t_i =5 nm (SiO_2 sample).

dC_{stray}/dV is nearly independent of the direct-current (dc) voltage in the sweep-voltage region between accumulation and inversion,[13] Eq. (3) can finally be simplified to

$$V_{sensor} \sim \frac{1}{C_{stray}} \frac{dC_{tip}}{dV} + \frac{const}{C_{stray}}. \quad (4)$$

Equation (4) estimates, in a first approximation, the influence of C_{stray} on the SCM signal. The output signal V_{sensor} is proportional to the derivative dC_{tip}/dV of the tip-sample capacitance C_{tip}. However, two components, $1/C_{stray}$ and $const/C_{stray}$, affect the signal of interest. As an example, Fig. 1 shows two dC/dV-V curves measured on two different locations of a stripe with a film thickness of 5 nm (SiO_2 sample). The locations were chosen to be far from each other (at the center and at the edge of the sample) in order to demonstrate a distinctly different C_{stray} in the different measurement positions. As can be seen, both curves differ significantly, which can only be due to the different values of C_{stray} for the different locations. The component $const/C_{stray}$ in Eq. (4) leads to a vertical shift (offset) of the dC/dV-V curves with respect to the sensor output axis and can be subtracted from the raw SCM data. On the other hand, the factor $1/C_{stray}$ in Eq. (4) influences the signal of interest dC_{tip}/dV. As shown in Fig. 1, the dC/dV peak area of the curve measured at the edge of the sample (low C_{stray}) is larger by a factor of about 1.8 than the dC/dV peak area of the curve measured in the center of the sample (large C_{stray}).

B. Dependence of the SCM signal on the film thickness

In order to minimize the effect of C_{stray}, the SCS measurements in our experiments were carried out on locations very close to the thickness-transition steps [i.e., 5.3/9.6, 9.6/14.5, and 14.5 nm/19.0 nm; see the inset of Fig. 2(a)]. The experience shows that C_{stray} does not significantly alter when the distance between the measurement points and also the movement of the probe is in the micrometer range, i.e., C_{stray} for pair positions "1" and "2," "3" and "4," as well as "5" and "6," should be nearly equal for each pair position [see the inset of Fig. 2(a)], but the output signal should be different due to the different oxide thicknesses. Thus, it should be possible to provide even a quantitative comparison between the dC/dV-V characteristics measured at locations with different oxide thicknesses nearby.

In order to allow a correlation between SCS data and conventionally measured or simulated C-V curves for the investigated film thicknesses of this work, the measured dC/dV-V characteristics were appropriately normalized. The following procedure, described in Fig. 2, was used to normalize the measured dC/dV-V curves.

(1) The "vertical offset" of the dC/dV-V characteristics [in a first approximation caused by the factor $const/C_{stray}$ in Eq. (4)] was subtracted from all raw SCS data.
(2) Assuming ideal oxide properties and identical oxide thicknesses in positions 2 and 3 (9.6 nm), the capacitance C_{tip} in these locations should be equal and the corresponding dC/dV-V characteristic should have identical dC/dV peak areas (A_{pos2}=A_{pos3} and A_{pos4}=A_{pos5}) because each dC/dV peak area is proportional to $C_{max}-C_{min}$, but only when C_{stray} in both measurement positions is identical [see Eq. (4)]. However, as discussed in detail, C_{stray} can be different for measurements at different locations. Therefore, to equal C_{stray} for positions 3 and 4, the dC/dV-V characteristic measured in position 3 is normalized with a factor f_1=A_{pos2}/A_{pos3}. Thus, after the normalizing procedure, the peak area of the dC/dV-V characteristic measured in position 3, referred to as A_{pos3} (normalized), is equal to the dC/dV peak area A_{pos2} [see Fig. 2(b)].

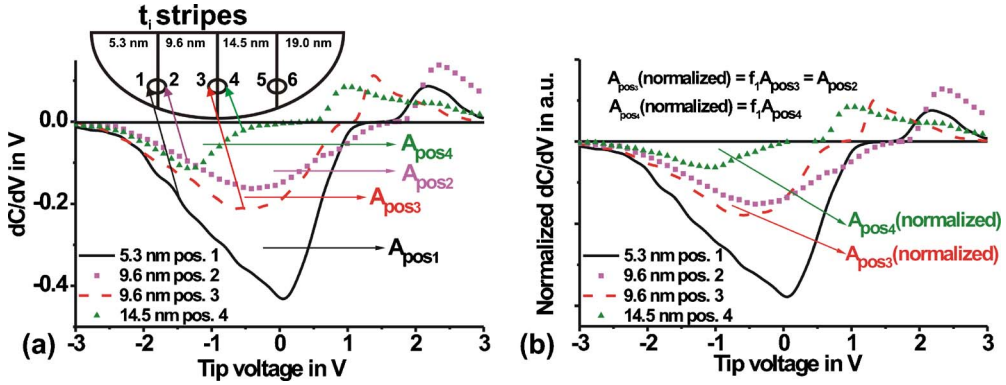

FIG. 2. (Color online) Normalizing procedure: (a) measured dC/dV-V characteristics before normalizing and (b) dC/dV-V curves after normalizing; inset of (a) locations of the SCS measurements.

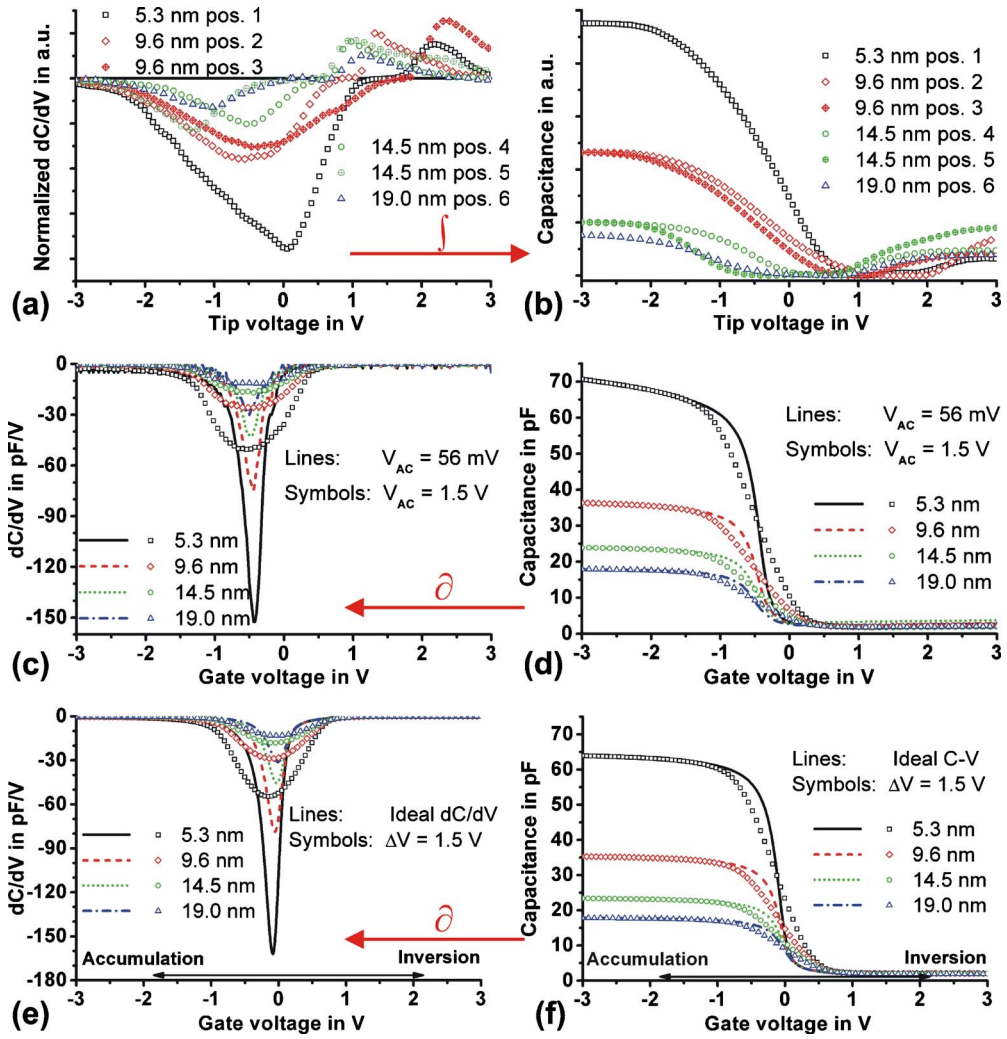

FIG. 3. (Color online) (a) Normalized (by peak area) dC/dV-V characteristics for SiO_2 films with different t_i (5.3, 9.6, 14.5, and 19.0 nm). (b) Corresponding calculated integrals (C-V curves). (c) Calculated derivatives of conventionally measured C-V curves for the SiO_2 films with different t_i (lines: V_{ac}=56 mV and symbols: V_{ac}=1.5 V). (d) Conventionally measured C-V curves for the SiO_2 films with different t_i (lines: V_{ac}=56 mV and symbols: V_{ac}=1.5 V). (e) Calculated derivatives of simulated C-V characteristics for the SiO_2 films with different t_i (lines: ideal and symbols: ΔV=1.5 V). (f) Simulated ideal C-V characteristics for the SiO_2 films with different t_i (lines: ideal and symbols: ΔV=1.5 V). Locations of the dC/dV-V measurements can be seen in Fig. 2.

(3) As mentioned above, if the experimenter works carefully, the C_{stray} between positions 3 and 4 should nearly be equal. Therefore, the dC/dV-V signal in position 4 can also be normalized by the factor f_1. The resulting dC/dV area is referred to as A_{pos4} (normalized).
(4) This was preceded in a similar way for the dC/dV-V characteristics measured in positions 5 and 6. They were normalized by factor $f_2=A_{pos4}(\text{normalized})/A_{pos5}$ (identical oxide thickness in positions 4 and 5 and nearly identical C_{stray} in positions 5 and 6). All normalized dC/dV-V curves for all film thicknesses are shown in Fig. 3(a).

Thereafter, the normalized dC/dV-V characteristics were integrated, and the resulting integral curves were shifted to equal C_{min} (in a first approximation, C_{min} is constant for different film thicknesses, but equal doping concentrations). The conventionally measured, as well as simulated, C-V characteristics were differentiated. The resulting C-V and dC/dV-V curves are represented in Fig. 3. The "tip voltage" in Figs. 1, 2, 3(a), and 3(b) is the typically used gate voltage with respect to the grounded substrate for MIS capacitors in conventional measurements.

The shifts between the dC/dV-V curves measured by SCS and the derivatives of conventionally measured C-V curves are mainly due to the work-function difference between the two electrode materials [for TiN electrodes, it is 4.2–4.3 eV,[19] and for Pt/Ir tips, it is 5.5 eV (Ref. 20)], but also due to different Q_{Is}. As expected, the slopes of the C-V curves measured with V_{ac} of 1.5 V are smaller than the slopes of the C-V characteristics measured with V_{ac} of 56 mV [Fig. 3(d)]. Therefore, in Fig. 3(c), the peaks of the derivatives of C-V curves with V_{ac} of 1.5 V are significantly broader but smaller than the peaks of the derivatives of C-V curves with V_{ac} of 56 mV. A similar behavior can be observed between the simulated ideal characteristics and the corresponding curves modulated with a ΔV of 1.5 V [Figs. 3(e) and 3(f)]. A neg-

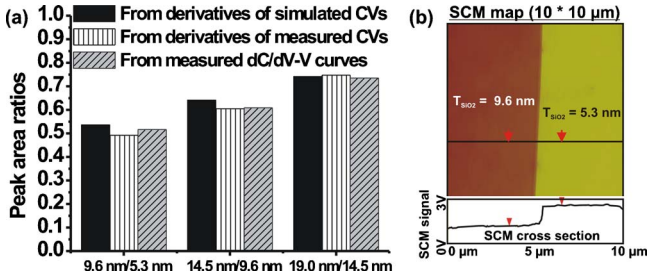

FIG. 4. (Color online) (a) Calculated peak area ratios between SiO_2 films with different thicknesses for measured dC/dV-V characteristics and for derivatives of measured, as well simulated, C-V characteristics and (b) SCM map (100 μm^2) and cross-section measured at the transition between different SiO_2 thicknesses as indicated in the figure (setting parameters are $V_{dc}=0$ V, $V_{ac}=1$ V, and $f_{dc}=90$ kHz).

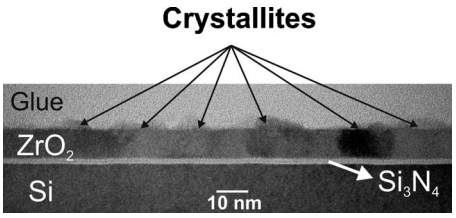

FIG. 5. HR-TEM picture of ZrO_2 high-k layer stacks.

ligible smaller slope of the measured C-V curves ($V_{ac}=56$ mV and $V_{ac}=1.5$ V) in Fig. 3(d) compared to the corresponding simulated C-V curves (ideal and modulated with a ΔV of 1.5 V) in Fig. 3(f) can also be observed, which could be explained by the existence of D_{it} (in the range of 5×10^{10} cm^{-2} eV^{-1}) for the experimental sample. Therefore, calculated derivatives of measured C-V characteristics [Fig. 3(c)] indicate slightly broader dC/dV peaks than the corresponding derivatives of simulated curves [Fig. 3(e)]. In comparison, measured dC/dV-V curves [with $V_{ac}=1.5$ V, Fig. 3(a)] show broader peaks than derivatives of measured [with $V_{ac}=1.5$ V, Fig. 3(c)] or simulated C-V curves modulated with a ΔV of 1.5 V [Fig. 3(e)]. Analogically, the corresponding integrals of measured dC/dV-V curves [Fig. 3(b)] show smaller slopes compared to the corresponding measured or simulated C-V characteristics [Figs. 3(d) and 3(f)]. This fact can be explained with the difference between large-area conventional C-V measurements and SCM measurements at the nanoscale, where the tip geometry strongly influences the dC/dV signal and leads to broadening of the peak of dC/dV-V curves.[17,21] Another difference is the small opposite peak (at positive tip voltages) in the measured dC/dV-V characteristics [Fig. 3(a)], which is negligible in the derivatives of the measured C-V characteristics and cannot be observed in the calculated derivatives of the simulated C-V curves. One potential reason for this effect might be the humidity in the atmosphere around the measurement setup because all experiments in our study were performed under ambient conditions. This may lead to the adsorption of water molecules on the sample surface, which can be charged and thus modify the measurement signal.[10] As the ratio of the "gate diameter" (i.e., the surrounding area around the "gate") to the gate area is significantly larger for SCM (the tip contact area is about 100 nm^2) compared to conventional C-V measurements (the gate contact area is 0.01 mm^2), this effect would be much more pronounced for SCM, as observed.

The most important fact, however, is that the increase in the dC/dV signal correlates quantitatively nearly perfect with the decreasing SiO_2 thicknesses. This becomes obvious in Fig. 4(a), where a very good agreement of the peak area ratios between the different film thicknesses for measured dC/dV-V curves and for the derivatives of conventionally measured ($V_{ac}=56$ mV), as well as simulated, ideal C-V characteristics was found.

SCM maps were also recorded across the transition regions between the different oxide thicknesses. As an example, a SCM map for stripes with thicknesses of 5.3 and 9.6 nm is shown in Fig. 4(b), together with a cross-section of the SCM signal. As can be seen, a pronounced SCM signal difference of about 1.5 V between the two regions with various film thicknesses can clearly be observed, which gives an estimation of the sensitivity of SCM for the detection of local variations of dielectric-layer thicknesses.

C. Sensitivity of SCM to small variations in film thickness at the nanoscale

Next, the sensitivity of SCM to the surface roughness caused by spatial variations in film thickness is demonstrated for the ZrO_2 high-k layer stacks. In Fig. 5, HR-TEM images clearly show that the interface between the ZrO_2 and the interfacial Si_xN_y (as well as the Si/Si_xN_y interface) is very smooth, whereas the ZrO_2 surfaces show relatively high roughness due to the crystallization (crystallites are clearly visible). Therefore, the surface roughness can be directly correlated with local thickness variations of the high-k layer and, thus, the whole dielectric stack.

Figure 6 shows the topography map and the simultaneously obtained SCM image of the crystalline high-k ZrO_2 layers together with cross sections. By a direct correlation of both maps, it is clearly visible that bright dots in the surface topography map [Fig. 6(a)] indicating crystallites with higher topography correspond exactly to dark dots in the SCM map [Fig. 6(b)] indicating locations with lower dC/dV signal (lower differential capacitance), i.e., the signal variations in the SCM image are caused by differences in film thickness and the thicker the film, the lower the dC/dV signal. Especially, in the cross-section images (Fig. 6, top), this behavior is obvious. For these ZrO_2 films with a thickness of about 10 nm, a difference in film thickness of about 2 nm results in a pronounced change in the differential capacitance. These results clearly prove the applicability of SCM for local film thickness mapping at the nanometer scale and for a qualitative determination of thickness variations. This high sensitivity of SCM to the surface roughness caused by film thickness variations is advantageous for the determination of film uniformity and/or morphology. Relatively rough surfaces, however, can lead to difficulties in the accurate determination of

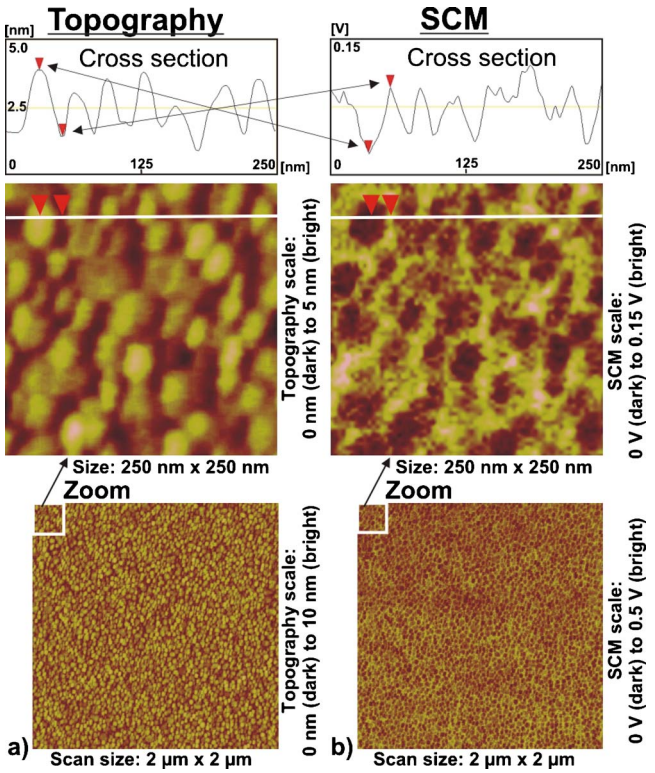

FIG. 6. (Color online) (a) Topography (rms roughness=0.85 nm) and (b) SCM map of ZrO_2 samples (dc bias is 0 V and ac amplitude is 4 V).

other layer characteristics (e.g., D_{it}) because both factors t_i and D_{it} can influence the dC/dV signal simultaneously.

IV. SUMMARY AND CONCLUSIONS

The capability of SCM to detect small changes in film thickness and for film thickness mapping at a nanoscale was demonstrated. The influence of most important layer characteristics (t_i, D_{it}, and Q_{Is}) on the SCM signal was discussed. The influence of C_{stray} on the SCM signal was also discussed and considered in the evaluation procedures. Thus, peak areas of measured dC/dV-V curves can quantitatively be compared with peak areas of derivatives of conventionally measured, as well as simulated, C-V characteristics for different film thicknesses. It was demonstrated that the dC/dV signal measured by SCS changes correlates directly with the insulator thickness. However, stray capacitance remains as the key parasitic factor that makes the quantification of SCM measurements performed after distinct movements of the probe challenging. Spatial variations of the dC/dV signal in the SCM map of crystalline high-k ZrO_2 films could be directly attributed to the corresponding topography. These results reveal SCM as a feasible tool for the detection of very small changes in film thickness at the nanoscale and for characterization of surface roughness caused by film thickness variations.

[1] C. C. Williams, Annu. Rev. Mater. Sci. **29**, 471 (1999).
[2] A. C. Diebold, M. R. Kump, J. J. Kopanski, and D. G. Seiler, J. Vac. Sci. Technol. B **14**, 196 (1996).
[3] Y. Huang, C. C. Williams, and J. Slinkman, Appl. Phys. Lett. **66**, 344 (1995).
[4] Y. Hong, Y. Yeow, W. Chim, K. Wong, and J. Kopanski, IEEE Trans. Electron Devices **51**, 1496 (2004).
[5] O. Bowallius and S. Anand, Mater. Sci. Semicond. Process. **4**, 81 (2001).
[6] K. Mang, Y. Kuk, J. Kwon, Y. Kim, D. Jeon, and C. Kang, Europhys. Lett. **67**, 261 (2004).
[7] R. Beyer and B. Schmidt, Microelectron. Eng. **84**, 376 (2007).
[8] D. Goghero, V. Raineri, and F. Giannazzo, Appl. Phys. Lett. **81**, 1824 (2002).
[9] J. Yang and F. C. J. Kong, Appl. Phys. Lett. **81**, 4973 (2002).
[10] T. Yamamoto, Y. Suzuki, H. Sugimura, and N. Nakagiri, Jpn. J. Appl. Phys., Part 1 **35**, 3793 (1996).
[11] D. K. Schroder, *Semiconductor Material and Device Characterization*, 3rd ed. (Wiley, Tempe, 2006), p. 321.
[12] R. C. Palmer, E. J. Deninger, and H. Kawamoto, RCA Rev. **43**, 194 (1982).
[13] G. H. Buh, C. Tran, and J. J. Kopanski, J. Vac. Sci. Technol. B **22**, 417 (2004).
[14] D. T. Lee, J. P. Pelz, and B. Bhushan, Rev. Sci. Instrum. **73**, 3525 (2002).
[15] J. J. Kopanski, J. F. Marchiando, B. G. Rennex, D. Simons, and Q. Chau, J. Vac. Sci. Technol. B **22**, 399 (2004).
[16] Š. Lányi, Ultramicroscopy **103**, 221 (2005).
[17] D. M. Schaadt and E. T. Yu, J. Vac. Sci. Technol. B **20**, 1671 (2002).
[18] J. Yang, A. Postula, and M. Bialkowski, Proc. SPIE **5274**, 543 (2004).
[19] F. Fillot, T. Morel, S. Minoret, I. Matko, S. Maitrejean, B. Guillaumot, B. Chenevier, and T. Billon, Microelectron. Eng. **82**, 248 (2005).
[20] J. W. G. Wildöer, C. J. P. M. Harmans, and H. van Kempen, Phys. Rev. B **55**, R16013 (1997).
[21] C. Eckhardt, W. Brezna, O. Bethge, E. Bertagnolli, and J. Smoliner, J. Appl. Phys. **105**, 113709 (2009).